Inorg. Chem. **2009**, *48*, 1689−1698

Inorganic Frameworks from Selenidotetrelate Anions $[T_2Se_6]^{4-}$ (T = Ge, Sn): Synthesis, Structures, and Ionic Conductivity of $[K_2(H_2O)_3][MnGe_4Se_{10}]$ and $(NMe_4)_2[MSn_4Se_{10}]$ (M = Mn, Fe)

Sima Haddadpour,[†] Maike Melullis,[†] Halgard Staesche,[†] C. R. Mariappan,[†] Bernhard Roling,[†] Rodolphe Clérac,[‡,§] and Stefanie Dehnen*[,†]

Fachbereich Chemie, Philipps-Universität Marburg, Hans-Meerwein-Strasse, 35043 Marburg, Germany, CNRS, UPR 8641, Centre de Recherche Paul Pascal (CRPP), Equipe "Matériaux Moléculaires Magnétiques", 115 avenue du Dr. Albert Schweitzer, Pessac F-33600, France, and Université de Bordeaux, UPR 8641, Pessac F-33600, France

Received November 12, 2008

Syntheses, structures, and physical properties of three inorganic framework compounds $[K_2(H_2O)_3][MnGe_4Se_{10}]$ (**1**), $(NMe_4)_2[MnSn_4Se_{10}]$ (**2**), and $(NMe_4)_2[FeSn_4Se_{10}]$ (**3**) are presented. The title compounds are based on a prominent open framework anionic structure; in these cases, however, they contain K^+, the smallest type of counterion to be included so far (**1**), or represent Sn analogues (**2**, **3**). Both changes with respect to related compounds are reflected in peculiar physical properties, such as ion conductivity or relatively small band gaps.

Introduction

The development of novel inorganic polymers that represent robust porous frameworks is studied by inorganic and material chemists to discover new systems for a variety of purposes. Among the technically most relevant targets are network compounds for selective gas storage[1−10] or heterogeneous catalysis,[11−16] and novel ion conductor materials for application as solid state electrolytes or separators in novel ion batteries.[17,18] Although lithium ion batteries are already widely used, the problems that are correlated to their thermal instabilities[19,20] prompted the search for alternatives.

Purely inorganic coordination polymers that are observed as anionic strands, layers, or framework substructures of corresponding salts are usually prepared by solvothermal techniques[21−23] or via the alkali metal polychalcogenide flux

* To whom correspondence should be addressed. E-mail: dehnen@chemie.uni-marburg.de. Fax: int + (0)6421 282 5751.
† Philipps-Universität Marburg.
‡ CNRS, CRPP.
§ Université de Bordeaux.

(1) (a) Liu, J. C.; Lee, J. Y.; Pan, L.; Obermyer, R. T.; Simizu, S.; Zande, B.; Li, J.; Sankar, S. G.; Johnson, J. K. *J. Phys. Chem. C* **2008**, *112*, 2911–2917. (b) Lee, J. Y.; Olson, D. H.; Pan, L.; Emge, T. J.; Li, J. *Adv. Funct. Mater.* **2007**, *17*, 1255–1262. (c) Park, H. S.; Britten, J. F.; Mueller, U.; Lee, J. Y.; Li, J. *Chem. Mater.* **2007**, *19*, 1302–1308. (d) Krungleviciute, V.; Lask, K.; Heroux, L.; Migone, A. D.; Lee, J.-Y.; Li, J.; Skoulidas, A. *Langmuir* **2007**, *23*, 3106–3109. (e) Pan, L.; Parker, B.; Huang, X. Y.; Olson, D. H.; Lee, J.-Y.; Li, J. *J. Am. Chem. Soc.* **2006**, *128*, 4180. (f) Pan, L.; Olson, D. H.; Ciemnolonski, L. R.; Heddy, R.; Li, J. *Angew. Chem., Int. Ed.* **2006**, *45*, 616. (g) Lee, J.-Y.; Li, J.; Jagiello, J. *J. Solid State Chem.* **2005**, *178*, 2527. (h) Lee, J.-Y.; Pan, L.; Kelly, S. K.; Jagiello, J.; Emge, T. J.; Li, J. *Adv. Mater.,* **2005**, *17*, 2703. (i) Pan, L.; Sander, M. B.; Huang, X.-Y.; Li, J.; Smith, M.; Bittner, E.; Bockrath, B.; Johnson, J. K. *J. Am. Chem. Soc.* **2004**, *126*, 1308. (j) Pan, L.; Liu, H.-M.; Lei, X.-G.; Huang, X.-Y.; Olson, D. H.; Turro, N. J.; Li, J. *Angew. Chem., Int. Ed.* **2003**, *42*, 542.

(2) (a) Wong-Foy, A. G.; Matzger, A. J.; Yaghi, O. M. *J. Am. Chem. Soc.* **2006**, *128*, 3494. (b) Rowsell, J. L. C.; Yaghi, O. M. *J. Am. Chem. Soc.* **2006**, *128*, 1304. (c) Rowsell, J. L. C.; Yaghi, O. M. *Angew. Chem., Int. Ed.* **2005**, *44*, 4670. (d) Ni, Z.; Yassar, A.; Antoun, T.; Yaghi, O. M. *J. Am. Chem. Soc.* **2005**, *127*, 12752. (e) Rowsell, J. L. C.; Millward, A. R.; Park, K. S.; Yaghi, O. M. *J. Am. Chem. Soc.* **2004**, *126*, 5666. (f) Yaghi, O. M.; O'Keefe, M.; Ockwig, N. W.; Chae, H. K.; Eddaoudi, M.; Kim, J. *Nature* **2003**, *423*, 705. (g) Rosi, N. L.; Eckert, J.; Eddaoudi, M.; Vodak, D. T.; Kim, J.; O'Keeffe, M.; Yaghi, O. M. *Science* **2003**, *300*, 1127. (h) Eddaoudi, M.; Kim, J.; Rosi, N.; Vodak, D.; Wachter, J.; O'Keeffe, M.; Yaghi, O. M. *Science* **2002**, *295*, 469. (i) Eddaoudi, M.; Kim, J.; Wachter, J. B.; Chae, H. K.; O'Keeffe, M.; Yaghi, O. M. *J. Am. Chem. Soc.* **2001**, *123*, 4368.

(3) Li, Y.; Yang, R. T. *J. Am. Chem. Soc.* **2006**, *128*, 726.

(4) (a) Chun, H.; Dybtsev, D. N.; Kim, H.; Kim, K. *Chem.—Eur. J.* **2005**, *11*, 3521. (b) Dybtsev, D. N.; Chun, H.; Kim, K. *Angew. Chem., Int. Ed.* **2004**, *43*, 5033. (c) Dybtsev, D. N.; Chun, H.; Yoon, S. H.; Kim, D.; Kim, K. *J. Am. Chem. Soc.* **2004**, *126*, 32.

(5) Kesanli, B.; Cui, Y.; Smith, M. R.; Bittner, E. W.; Bockrath, B. C.; Lin, W. *Angew. Chem., Int. Ed.* **2005**, *44*, 72.

(6) (a) Dinca, M.; Long, J. R. *J. Am. Chem. Soc.* **2005**, *127*, 9376. (b) Kaye, S. S.; Long, J. R. *J. Am. Chem. Soc.* **2005**, *127*, 6506.

(7) (a) Matsuda, R.; Kitaura, R.; Kitagawa, S.; Kubota, Y.; Belosludov, R. V.; Kobayashi, T. C.; Sakamoto, H.; Chiba, T.; Takata, M.; Kawazoe, Y.; Mita, Y. *Nature* **2005**, *436*, 238. (b) Lee, E. Y.; Jang, S. Y.; Suh, M. P. *J. Am. Chem. Soc.* **2005**, *127*, 6374. (c) Kubota, Y.; Takata, M.; Matsuda, R.; Kitaura, R.; Kitagawa, S.; Kato, K.; Sakata, M.; Kobayashi, T. C. *Angew. Chem., Int. Ed.* **2005**, *44*, 920.

(8) (a) Snurr, R. Q.; Hupp, J. T.; Nguyen, S. T. *AIChE J.* **2004**, *50*, 1090. (b) Zhao, X.; Xiao, B.; Fletcher, A. J.; Thomas, K. M.; Bradshaw, D.; Rosseinsky, M. J. *Science* **2004**, *306*, 1012.

10.1021/ic802170f CCC: $40.75
Published on Web 01/21/2009

method.[24] Most of the respective phases represent chalcogenidometallate compounds of main group (semi)metals, transition metals, or a combination of both with the general formulas $A_q[M_xT_yE_z]$ or $A_q[M_xM'_yT_z]$ (A = alkali(ne earth) metal; T = Group 13, 14, 15 (semi)metal; M, M′ = transition metal; E = S, Se, Te). For a typical preparation procedure, a mixture of simple salts or a mixture of the elements is reacted at appropriate temperatures in supercritical solvent suspensions or in an excess polychalcogenide melt, directing the product composition mainly by the basicity of the mixture. Some of the compounds, like metal derivatives of group 14 metallates (= tetrelates) $[A_2(H_2O)_n][MGe_4E_{10}]$ (A = NMe_4, Rb, Cs; M = Mn, Fe, Cu_2, Ag_2, Ag; E = S, Se)[25] can be viewed as "diluted solids" with counterions occupying holes that have been driven into the underlying (semi)metal chalcogenide or represent zeolite-type topologies;[26] others, like $K_6\{Sn[Zn_4Sn_4S_{17}]\}$[27] or $K_6[M_4Sn_3Se_{13}]$ (M = Zn, Cd),[28a,c,e] show no structural relationship to any main group or transition metal chalcogenide. However, because of their composition and structures, all of these salts combine interesting opto-electronic or magnetic properties, in the presence of open d-shell transition metal atoms, with the porous nature of a zeolite.

An alternative route into multinary chalcogenide phases is a coordination chemistry approach, that is, reactions in solvent under ambient conditions.[29] Here, binary anions $[T_xE_y]^{q-}$ are reacted with transition metal ions M^{n+}. The resulting phases are also based on anionic, chalcogen bridged heterobimetallic complexes, that is, mixed metal chalcogenidometallate anions. In contrast to the solvothermal or flux method, most of the products evolving from these experiments contain molecular anionic complexes, like $[M_4T_4E_{17}]^{10-}$ (M = Mn, Fe, Co, Ni, Zn, Cd, Hg; T = Ge, Sn; E = S, Se, Te),[30,28b,d] $[M_5Sn_5S_{20}]^{10-}$ (M = Zn, Co)[31] or $[Mn_6(H_2O)_6Ge_4Se_{17}]^{6-}$,[32] whereas extended anions, such as $^1_\infty\{[MSnE_4]^{2-}\}$ (A = K, Cs; M = Hg, Mn; E = Se, Te),[33,28b] $^2_\infty\{[Mn_6(H_2O)_3Ge_4Se_{17}]^{6-}\}$,[32] or $^3_\infty\{[Hg_4Sn_3Te_{13}]^{6-}\}$[28d] are observed less frequently.

Herein we report on the extension of the $^3_\infty\{[MT_4E_{10}]^{2-}\}$ open framework compounds to the potassium salt $[K_2(H_2O)_3][MnGe_4Se_{10}]$ (**1**), containing the smallest counterion within this anionic substructure, and the heavier homologues $(NMe_4)_2[MnSn_4Se_{10}]$ (**2**), and $(NMe_4)_2[FeSn_4Se_{10}]$ (**3**), that belong to the first stannates to be based on this framework type—prepared at the same time as $(NMe_4)_2[MSn_4Se_{10}]$ (M =Mn, Fe, Co, Zn) but from another precursor.[34] The compounds are obtained as single crystals from reactions of selenidotetrelate salts $[K_4(H_2O)_2][Ge_2Se_6]$,[35]

(9) (a) Férey, G.; Latroche, M.; Serre, C.; Millange, F.; Loiseau, T.; Percheron-Guégan, A. *Chem. Commun.* **2003**, 2976. (b) Vishnyakov, A.; Ravikovitch, P. I.; Neimark, A. V.; Bulow, M.; Wang, Q. M. *Nano Lett.* **2003**, *3*, 713. (c) Pan, L.; Adams, K. M.; Hernandez, H. E.; Wang, X.; Zheng, C.; Hattori, Y.; Kaneko, K. *J. Am. Chem. Soc.* **2003**, *125*, 3062.

(10) (a) Siriwardane, R. V.; Shen, M. S.; Fisher, E. P. *Energy Fuels* **2003**, *17*, 571–576. (b) Seki, K.; Mori, W. *J. Phys. Chem. B* **2002**, *106*, 1380. (c) Ustinov, E. A.; Do, D. D. *Langmuir* **2002**, *18*, 3567–3577. (d) Chui, S.S.-Y.; Lo, S. M.-F.; Charmant, J. P. H.; Orpen, A. G.; Williams, I. D. *Science* **1999**, *283*, 1148. (e) Dubinin, M. M.; Astakhov, V. A. *Adv. Chem. Ser.* **1970**, *102*, 69.

(11) (a) Mueller, U.; Schubert, M.; Teich, F.; Puetter, H.; Schierle-Arndt, K.; Pastre, J. *J. Mater. Chem.* **2006**, *16*, 626. (b) Hermes, S.; Schroter, M. K.; Schmid, R.; Khodeir, L.; Muhler, M.; Tissler, A.; Fischer, R. W.; Fischer, R. A. *Angew. Chem., Int. Ed.* **2005**, *44*, 6237.

(12) (a) Zhang, Z.; Zhang, J.; Wu, T.; Bu, X.; Feng, P. *J. Am. Chem. Soc.* **2008**, *130*, 15238. (b) Zheng, N.; Bu, X.; Vu, H.; Feng, P. *Angew. Chem., Int. Ed.* **2005**, *44*, 5699–5303.

(13) (a) Wang, W.; Hunger, M. *Acc. Chem. Res.* **2008**, *41*, 895–904. (b) Jiang, Y.; Hunger, M.; Wang, W. *J. Am. Chem. Soc.* **2006**, *128*, 11679–11692. (c) Marthala, V. R. R.; Jiang, Y.; Huang, J.; Wang, W.; Glaser, R.; Hunger, M. *J. Am. Chem. Soc.* **2006**, *128*, 14812–14813.

(14) (a) Cheng, Y.; Hoard, J.; Lambert, C.; Kwak, J. H.; Peden, C. H. F. *Catal. Today* **2008**, *136*, 34–39. (b) Lei, C.; Soares, T. A.; Shin, Y.; Liu, J.; Ackerman, E. J. *Nanotechnology* **2008**, *19*, 125102.

(15) (a) Pan, L.; Olson, D. H.; Ciemnolonski, L. R.; Heddy, R.; Li, J. *Angew. Chem., Int. Ed.* **2006**, *45*, 616. (b) Pan, L.; Adams, K. M.; Hernandez, H. E.; Wang, X. T.; Zheng, C.; Hattori, Y.; Kaneko, K. *J. Am. Chem. Soc.* **2003**, *125*, 3062.

(16) (a) Schlichte, K.; Kratze, T.; Kaskel, S. *Microporous Mesoporous Mater.* **2004**, *73*, 81. (b) Velu, S.; Wang, L.; Okazaki, M.; Suzuki, K.; Tomura, S. *Microporous Mesoporous Mater.* **2002**, *54*, 113–126. (c) Lin, K.-S.; Wang, H. P. *Appl. Catal., B* **1999**, *22*, 261–267. (d) Becker, L.; Förster, H. *Appl. Catal., B* **1998**, *17*, 43–49.

(17) Kajihara, K.; Matsuishi, S.; Hayashi, K.; Hirano, M.; Hosono, H. *J. Phys. Chem. C* **2007**, *111*, 14855–14861.

(18) Zheng, N.; Bu, X.; Feng, P. *Nature* **2003**, *426*, 428–432.

(19) Yang, H.; Amiruddin, S.; Bang, H. J.; Sun, Y.-K.; Prakash, J. *J. Ind. Eng. Chem.* **2006**, *12*, 12–38.

(20) Sollmann, D. J. *Nachr. Chem.* **2007**, *55*, 979–983.

(21) (a) Feng, P.; Bu, X.; Zheng, N. *Acc. Chem. Res.* **2005**, *38*, 293–303. (b) Bu, X.; Zheng, N.; Feng, P. *Chem.—Eur. J.,* **2004**, *10*, 3356–3362. (c) Bu, X.; Zheng, N.; Li, Y.; Feng, P. *J. Am. Chem. Soc.* **2002**, *124*, 12646–12647. (d) Wang, C.; Bu, X.; Zheng, N.; Feng, P. *Angew. Chem., Int Ed.* **2002**, *41*, 1959–1961.

(22) Sheldrick, W. S.; Wachhold, M. *Angew. Chem., Int. Ed. Engl.* **1997**, *36*, 206–224.

(23) (a) Bedard, R. L.; Wilson, S. T.; Vail, L. D.; Bennett, J. M.; Flanigen E. M. In *Zeolites: Facts, Figures, Future. Proceedings of the 8th International Zeolite Conference*; Jacobs, P. A., van Santen, R. A., Eds.; Elsevier: Amsterdam, 1989; p 375.

(24) Kanatzidis, M. G.; Pöttgen, R.; Jeitschko, W. *Angew. Chem., Int. Ed. Engl.* **2005**, *44*, 6996–7023.

(25) (a) Yaghi, O. M.; Sun, Z.; Richardson, D. A.; Groy, T. L. *J. Am. Chem. Soc.* **1994**, *116*, 807. (b) Bowes, C. L.; Lough, A. J.; Malek, A.; Ozin, G. A.; Petrov, S.; Young, D. *Chem. Ber.* **1996**, *129*, 283. (c) Bowes, C. L.; Huynh, W. U.; Kirkby, S. J.; Malek, A.; Ozin, G. A.; Petrov, S.; Twardowski, M.; Young, D.; Bedard, R. L.; Broach, R. *Chem. Mater.* **1996**, *8*, 2147. (d) Ahari, H.; Garcia, A.; Kirkby, S.; Ozin, G. A.; Young, D.; Lough, A. J. *J. Chem. Soc., Dalton Trans.* **1998**, 2023. (e) Loose, A.; Sheldrick, W. S. *Z. Naturforsch.* **1997**, *B 52*, 687.

(26) Cahill, C. L.; Parise, J. B. *Chem. Mater.* **1997**, *9*, 807.

(27) Manos, M. J.; Iyer, R. G.; Quarez, E.; Liao, J. H.; Kanatzidis, M. G. *Angew. Chem., Int. Ed.* **2005**, *44*, 3552–3555.

(28) (a) Ding, N.; Chung, D.-Y.; Kanatzidis, M. G. *Chem. Commun.* **2004**, 1170–1171. (b) Brandmayer, M. K.; Clérac, R.; Weigend, F.; Dehnen, S. *Chem.—Eur. J.* **2004**, *10*, 5147–5157. (c) Wu, M.; Su, W.-P.; Jasutkar, N.; Huang, X.-Y.; Li, J. *Mater. Res. Bull.* **2005**, *40*, 21. (d) Ruzin, E.; Fuchs, A.; Dehnen, S. *Chem. Commun.* **2006**, 4796–4798. (e) Wu, M.; Emge, T. J.; Huang, X.-Y.; Li, J.; Zhang, Y. *J. Solid State Chem.* **2008**, *181*, 415–422.

(29) Dehnen, S.; Melullis, M. *Coord. Chem. Rev.* **2007**, *251*, 1259–1280.

(30) (a) Lips, F.; Dehnen, S. *Inorg. Chem.* **2008**, *47*, 5561–5563. (b) Ruzin, E.; Jakobi, S.; Dehnen, S. *Z. Anorg. Allg. Chem.* **2008**, *634*, 995–100. (c) Ruzin, E.; Zimmermann, C.; Hillebrecht, P.; Dehnen, S. *Z. Anorg. Allg. Chem.* **2007**, *633*, 820–829. (d) Ruzin, E.; Dehnen, S. *Z. Anorg. Allg. Chem.* **2006**, *632*, 749–755. (e) Palchik, O.; Iyer, R. G.; Canlas, C. G.; Weliky, D. P.; Kanatzidis, M. G. *Z. Anorg. Allg. Chem.* **2004**, *630*, 2237–2247. (f) Dehnen, S.; Brandmayer, M. K. *J. Am. Chem. Soc.* **2003**, *125*, 6618–6619. (g) Palchik, O.; Iyer, R. G.; Liao, J. H.; Kanatzidis, M. G. *Inorg. Chem.* **2003**, *42*, 5052–5054. (h) Melullis, M.; Zimmermann, C.; Anson, C. E.; Dehnen, S. *Z. Anorg. Allg. Chem.* **2003**, *629*, 2325–2329. (i) Zimmermann, C.; Melullis, M.; Dehnen, S. *Angew. Chem., Int. Ed.* **2002**, *41*, 4269–4272.

(31) Zimmermann, C.; Anson, C. E.; Weigend, F.; Clérac, R.; Dehnen, S. *Inorg. Chem.* **2005**, *44*, 5686–5695.

(32) Melullis, M.; Clérac, R.; Dehnen, S. *Chem. Commun.* **2005**, 6008–6010.

(33) (a) Dhingra, S. S.; Haushalter, R. C. *Chem. Mater.* **1994**, *6*, 2376–2381. (b) Zimmermann, C.; Dehnen, S. *Z. Anorg. Allg. Chem.* **2003**, *629*, 1553–1556.

(34) Tsamourtzi, K.; Song, J.-H.; Bakas, T.; Freeman, A. J.; Trikalitis, P. N.; Kanatzidis, M. G. *Inorg. Chem.* **2008**, *47*, 11920.

Table 1. Crystallographic and Refinement Details of **1**−**4**[36] Measured at 100 K (IPDS II) or 193 K (IPDS I)

compound	**1**	**2**	**3**	**4**
empirical formula	$H_6Ge_4K_2MnO_3Se_{10}$	$H_{24}N_2C_8MnSn_4Se_{10}$	$H_{24}N_2C_8FeSn_4Se_{10}$	$C_{18}H_{56}N_4O_2Se_6Sn_2$
formula weight /g·mol^{-1}	1267.15	1467.59	1468.50	1071.81
crystal shape	truncated tetrahedon	truncated tetrahedon	truncated tetrahedon	block
crystal color	orange	cherry-red	black	yellow
crystal size /mm^3	0.80 × 0.80 × 0.80	0.55 × 0.30 × 0.30	0.10 × 0.10 × 0.08	0.80 × 0.75 × 0.60
diffractometer	Stoe IPDS II	Stoe IPDS I	Stoe IPDS II	Stoe IPDS I
radiation (λ /Å)	$Mo_{K\alpha}$ (0.71073)	$Mo_{K\alpha}$ (0.71073)	$Mo_{K\alpha}$ (0.71073)	$Mo_{K\alpha}$ (0.71073)
crystal system	tetragonal	tetragonal	tetragonal	monoclinic
space group	$I\bar{4}$ (No. 82)	$I\bar{4}$ (No. 82)	$I\bar{4}$ (No. 82)	$P2_1/n$ (No. 14)
a /Å	8.9880(13)	9.8647(14)	9.8785(14)	11.2068(22)
b /Å	8.9880(13)	9.8647(14)	9.8785(14)	9.7849(20)
c /Å	15.490(3)	15.317(3)	15.345(3)	17.6511(35)
β /deg				107.81(3)
V /Å^3	1251.3(4)	1490.5(4)	1497.4(4)	1842.8(6)
Z	2	2	2	2
ρ_{calc} /g·cm^{-3}	3.363	3.270	3.257	1.932
$\mu(Mo_{K\alpha})$ /mm^{-1}	20.113	15.928	15.92	7.30
2Θ range /deg	8−56	5−52	5−53	5−52
no. of measured reflections	5686	5186	2101	8723
no. of independent reflections	1507	1458	1099	3520
R(int)	0.0884	0.0731	0.0939	0.0535
no. of indep. reflections ($I > 2\sigma(I)$)	1357	1121	709	2203
no. of parameters	70	58	46	254
R_1 ($I > 2\sigma(I)$)	0.0399	0.0335	0.0615	0.0346
wR_2 (all data)	0.0865	0.0674	0.0614	0.0722
S (all data)	1.103	0.847	1.002	0.807
Flack parameter [36b]	0.00(5)	0.001(18)	0.02(3)	−
largest diff. peak/hole /e$^-$·10^{-6}pm^{-3}	0.775/−1.287	0.925/−0.688	0.955/−0.981	1.128/−0.917

or $(NMe_4)_4[Sn_2Se_6]$·2MeOH (**4**) with $MnCl_2$·4 H_2O or $Fe(OAc)_2$ in H_2O/MeOH mixtures at room temperature. By comparison of our investigations with former reactions, it is possible to gain insight into the aggregation tendencies of chalcogenidotetrelates in the presence of different transition metals and/or counterions. In addition to the structure elucidation of phases **1**−**4**, the compounds were investigated with respect to their optical absorption behavior. Compound **1**, containing the smallest cation (K^+) that ever served as a template for the generation of this type of open framework structure, and the NMe_4/Sn analogue **2** were particularly studied with respect to thermal behavior, ion mobility, and conductivity, which was studied by means of thermal gravimetry (TG)-differential scanning calorimetry (DSC) measurements and impedance spectroscopy.

Experimental Section

Syntheses. General Procedures. All reaction steps were performed with strong exclusion of air and external moisture (Ar atmosphere at a high-vacuum, double-manifold Schlenk line or N_2 atmosphere in a glovebox). Methanol, THF, and toluene were dried and freshly distilled prior to use; water was degassed by applying dynamic vacuum (10^{-3} Torr) for several hours.

Synthesis of $H_6O_3Ge_4K_2MnSe_{10}$ (1). A solution of 0.039 g (0.2 mmol) of $MnCl_2$·4H_2O in MeOH (5 mL) was added dropwise to a solution of 0.080 g (0.1 mmol) of $[K_4(H_2O)_3][Ge_2Se_6]$[35] in a mixture of MeOH (4.5 mL) and H_2O (0.5 mL) at room temperature, resulting in the immediate formation of a pale yellow solution and an orange precipitate. Upon stirring for 30 min the precipitate was filtered off. The filtrate was cooled down to −40 °C and layered by 10 mL of toluene, whereupon **1** was observed as large, orange crystals in a truncated tetrahedron shape after a few days. Yield of **1**: 0.026 g (0.021 mmol, 52% based on Ge). Elemental analysis (EDX) [atom % observed (calculated)]: K 11.45 (11.76), Mn 7.75 (5.88), Ge 24.63 (23.53), Se 56.16 (58.88).

Synthesis of $C_8H_{24}N_2MnSe_{10}Sn_4$ (2). A solution of 0.010 g (0.05 mmol) of $MnCl_2$·4H_2O in H_2O (5 mL) was added dropwise to a solution of 0.050 g (0.05 mmol) of $(NMe_4)_4[Sn_2Se_6]$·2MeOH (**4**) in MeOH (5 mL) at room temperature, resulting in the immediate formation of an intense orange solution and a flesh-colored precipitate. Upon stirring for 12 h the precipitate was removed by filtration. The filtrate was layered by 10 mL of THF, whereupon **2** was observed as aggregates of cherry-red crystals in a truncated tetrahedron shape after a few days. Yield of **2**: 0.021 g (0.014 mmol, 57% based on Sn). Elemental analysis (EDX) [atom % observed (calculated)]: Mn 5.88 (6.67), Sn 22.92 (26.67), Se 71.20 (66.67).

Synthesis of $C_8H_{24}N_2FeSe_{10}Sn_4$ (3). A solution of 0.014 g (0.05 mmol) of $FeSO_4$·7H_2O in H_2O (5 mL) was added dropwise to a solution of 0.050 g (0.05 mmol) of $(NMe_4)_4[Sn_2Se_6]$·2MeOH in MeOH (5 mL) at room temperature, resulting in the immediate formation of a dark solution and a black precipitate. Upon stirring for 12 h the precipitate was removed by filtration. The filtrate was layered by 10 mL of THF, whereupon **3** was observed as very small, black crystals in a truncated tetrahedron shape after a few days. Yield of **3**: 0.008 g (0.005 mmol, 22% based on Sn). Elemental analysis (EDX) [atom % observed (calculated)]: Fe 6.23 (6.67), Sn 24.82 (26.67), Se 69.00 (66.67).

Synthesis of $C_{18}H_{56}N_4O_2Se_6Sn_2$ (4). A solution of 6.6 g (0.01 mol) of $[K_4(H_2O)_4][SnSe_4]$[30b] in MeOH (200 mL) was layered by a saturated solution of NMe_4Cl (36.0 g, 0.33 mol) in 200 mL of MeOH at room temperature. **4** precipitated instantly as bright yellow blocks that have been washed by NMe_4Cl solution and dried. Yield of **4**: 5.1 g (0.009 mol, 95% based on Sn). Elemental analysis (EDX) [atom % observed (calculated)]: Sn 23.66 (25.00), Se 76.33 (75.00).

Crystal Structure Analyses. All data were collected on diffractometers equipped with Stoe imaging plate detector systems IPDS I (**2**, **4**) or IPDS-II (**1**, **3**), using $Mo_{K\alpha}$ radiation and graphite monochromatization (λ = 0.71073 Å) at T = 193

K (**1**, **3**) or $T = 203$ K (**1**, **4**). Structure solution and refinement were performed using the Shelxs-97 and Shelxl-97 software.[36] Table 1 summarizes the crystallographic data, structure solution, and refinement details. **1**: refinement of Mn, Ge, Se, two of three O atomic positions and two of three K split positions employing anisotropic displacement parameters; the K atomic position 3-fold disordered, one O atomic position 2-fold disordered; refinement of respective split positions for O and one of the K split positions employing isotropic displacement parameters; H atoms not calculated. **2**: refinement of Mn, Ge, Se, N, C atomic positions employing anisotropic displacement parameters; H atoms calculated as riding on a pivot atom. **3**: refinement of Fe, Ge, Se, N, C atomic positions employing anisotropic displacement parameters; H atoms calculated as riding on a pivot atom. **4**: refinement of Fe, Ge, Se atomic positions employing anisotropic displacement parameters; refinement of N and C atoms employing isotropic displacement parameters; H atoms calculated as riding on a pivot atom. Further details of the crystal structure investigation for compound **1** can be obtained from the Fachinformationszentrum Karlsruhe, 76344 Eggenstein-Leopoldshafen, Germany, (fax: +49 7247−808−666; e-mail: crysdata@fiz−karlsruhe.de) on quoting the depository number CSD 419968. CCDC 705518−705520 contain the supplementary crystallographic data for compounds **2**, **3**, and **4** in this paper. These data can be obtained free of charge via ww.ccdc.cam.ac.uk/data_request/cif, or by emailing data_request@ccdc.cam.ac.uk, or by contacting The Cambridge Crystallographic Data Centre, 12, Union Road, Cambridge CB2 1EZ, U.K.; fax: +44 1223 336033.

UV−vis Spectroscopy. The UV−vis spectra of suspensions of single crystals in nujol oil between two quartz plates were recorded using a Varian Cary 5000 spectrometer in the range 200−800 nm and a scan rate of 200 nm·min^{-1}.

Magnetic Measurements. The magnetic susceptibility measurements were obtained using a Quantum Design SQUID magnetometer MPMS-XL housed at the Centre de Recherche Paul Pascal. This magnetometer works between 1.8 and 400 K for direct current (dc) applied fields ranging from −7 to 7 T. Measurements were performed on a 14.7 mg polycrystalline sample. The samples were handled under argon atmosphere and sealed in a plastic bag to avoid any contact with air or water. The presence of ferromagnetic impurities was excluded by measuring the field dependency of the magnetization at 100 K. The magnetic data were corrected for the sample holder and the diamagnetic contributions.

Impedance Spectroscopy. Polycrystalline pellets were prepared under N_2 atmosphere in a glovebox (MBraun, Unilab, <0.1 ppm O_2, <0.1 ppm H_2O) by employment of a hydraulic press, applying a pressure of approximately 3 bar. The pellets were sandwiched between conducting polymer electrodes (EMI-tec AS61) and mounted into an airtight sample cell. The alternating current (ac) impedance measurements were carried out in a frequency range from 0.1 Hz to 1 MHz at temperatures between 20 and 220 °C using a Novocontrol Alpha-AK impedance analyzer. Rms ac voltages of typically 0.5 V were applied to the samples. The sample temperature was controlled by the Novocontrol Quatro Cryosystem.

Thermal Gravimetric Analyses. TGA and DSC measurements were performed at single crystalline material by means of a TGA/SDTA851 and a DSC/821 instrument, both of Mettler Toledo, between room temperature and 800 °C.

Scheme 1. Overview or Syntheses of Compounds **1**−**3** by Reaction of Selenidotetrelate Salts with Transition Metal Salts in a H_2O/MeOH Mixture under Inert Conditions[a]

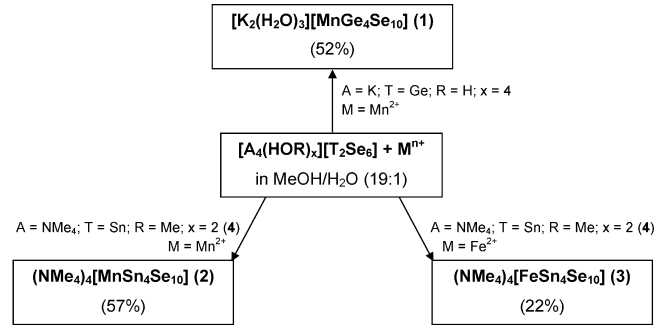

[a] The reaction mixtures were worked up by filtration from different amounts of precipitated MSe; crystallization of the products was obtained upon layering by toluene (**1**) or THF (**2**, **3**), respectively.

Results and Discussion

Syntheses. Quaternary chalcogenidometallate compounds $[K_2(H_2O)_3][MnGe_4Se_{10}]$ (**1**), $(NMe_4)_2[MnSn_4Se_{10}]$ (**2**), and $(NMe_4)_2[FeSn_4Se_{10}]$ (**3**) were prepared by reactions of selenidotetrelate salts $[K_4(H_2O)_2][Ge_2Se_6]$ or $(NMe_4)_4[Sn_2Se_6]\cdot 2MeOH$ (**4**) with $MnCl_2$ or $Fe(OAc)_2$, respectively, in water/methanol mixtures, as shown in Scheme 1 and outlined in more detail in the Experimental Section. All compounds were isolated as single crystals upon layering of the mother liquors by toluene (**1**) or THF (**2**, **3**), respectively, and structurally characterized by means of single crystal X-ray diffractometry. Compound **4** was obtained and crystallized upon layering a solution of $[K_4(H_2O)_4][SnSe_4]$[37] in methanol by a saturated MeOH solution of NMe_4Cl. Further investigations were followed up on pure single crystals. Pictures of the truncated tetrahedral crystals of **1**−**3** are presented in Figure 1.

The results of the reactions clearly indicate the crucial role of the cations during the aggregation of chalcogenidotetrelate anions and their reactivity toward transition metal ions in solution: whereas Ba^{2+} ions give rise for the formation of highly hydrated, water-coordinated, molecular Mn/Ge/Se anions, $[Mn_6(H_2O)_6Ge_4Se_{17}]^{6-}$ or a two-dimensional (2D) layer of identical, linked clusters, without changing the Ge/Se subunits,[32] we observe the aggregation of the starting material $[Ge_2Se_6]^{4-}$ into larger $[Ge_4Se_{10}]^{4-}$ anions that act as spacers between Mn^{2+} ions in a three-dimensional (3D) network during the reaction in the presence of K^+ ions, yielding **1**. For the Sn/Se combination, the so far examined alkali metal ions Na^+ to Cs^+ and Ba^{2+} led to the formation of molecular T3 or P1 type cluster anions, or the 3D linked variant of the latter upon reacting the selenidostannate salts with transition metal ions in solution—always maintaining the reacted Sn/Se subunit.[28b,30] Here, the bulky tetraalkylammonium counterions provoke or facilitate (i) the formation of a dimeric anion $[Sn_2Se_6]^{4-}$ at the preparation of the starting material from $[K_4(H_2O)_4][SnSe_4]$, according to the pH dependent equilibrium given in eq 1, and (ii) the further aggregation during the following reaction with Mn^{2+} (**2**) or Fe^{2+} (**3**).

(35) Melullis, M.; Dehnen, S. *Z. Anorg. Allg. Chem.* **2007**, *633*, 2159–2167.
(36) (a) Sheldrick, G. W. *SHELXTL*, v. 5.1; Bruker AXS Inc.: Madison, WI, 1997. (b) Flack, H. D. *Acta Crystallogr.* **1983**, *A39*, 876–881.
(37) Ruzin, E., PhD thesis, Philipps-Universität Marburg, Germany, 2007.

Figure 1. Photographs of near tetrahedral crystals of compounds **1** (left), **2** (center), and **3** (right). Approximate crystal sizes (given as largest diameter): 2.5 mm (**1**), 1.0 mm (**2**), 0.1 mm (**3**).

$$4[TE_4]^{4-} + 6H_2O \rightleftarrows 2[T_2E_6]^{4-} + 4HE^- + 4OH^- + 2H_2O \rightleftarrows [T_4E_{10}]^{4-} + 6HE^- + 6OH^- \quad (1)$$

Beside the desired realization of the most stable crystal packing with optimal fit of cationic and anionic sizes, which is obvious for the ammonium salt, another, more subtle influence on the formation of the ternary aggregates in solution is very likely. This is indicated by the reproducible formation of exclusively **1** without any hint for the formation of further ternary anions in solution as soon as K^+ is the only counterion available. Preliminary investigations by dynamic light scattering indicate that *in situ* existing Se···K···Se bridged subunits might contribute to control the product formation. This initial role is corroborated furthermore by the impact of the hydration requirements of the cations, which were previously shown to be crucial.[30b,d]

Crystal Structures. Title compounds **1**−**3** crystallize isotypically to known phases $[A_2(H_2O)_n][MGe_4E_{10}]$ (A = NMe_4, Rb, Cs; M = Mn, Fe, Co, Zn, Cu_2, Ag_2 Ag; E = S, Se, Te)[25,34] in the tetragonal space group $I\bar{4}$ with two formula units per unit cell. The isotypic situation accords with the same crystal shape as reported for microcrystals of $(NMe_4)_2[MGe_4S_{10}]$,[25b,c] or $(NMe_4)_2[MnSn_4Se_{10}]$,[34] that were, however, about several orders of magnitudes smaller than the crystals that we produced. It is worth mentioning that the cited ammonium salts, with the exception of $(NMe_4)_2[MnGe_4S_{10}]$,[25a] have exclusively been obtained as microcrystals; the respective crystal structure refinements have therefore been realized by Rietveld refinement of powder X-ray diffraction (XRD) data based on the single crystal structural data of the pioneer compound. As $[A_2(H_2O)_3][MnGe_4Se_{10}]$ (A = Rb, Cs),[25e] compound **1** contains three water molecules per formula unit, and the atomic positions of alkali metal ions and water molecules are disordered. This hint of a significant mobility of the counterions and for a possible exchange of solvent molecules has been the reason for a couple of further investigation discussed below. Figure 2 shows exemplarily (a) a fragment of the crystal structure of **1** considering all split positions of K and O atoms, (b) the topology of corner-linked $[Ge_4Se_{10}]$ T2 type supertetrahedra and $[MnSe_4]$ T1 tetrahedra, and (c) a polyhedral representation of the network in **1** emphasizing the relationship of both the ternary M/T/E framework (as represented by the barycenters of the $[MSe_4]$ and $[T_4Se_6]$ units) and the cavity/channel system within the anionic substructure to the diamond framework. Table 2 provides structural parameters of all compounds.

Details of the open framework sphalerite type arrangement of the 3D anions are not discussed in detail here, since the structure type is known in principle; only the topological relationship to the diamond lattice is referred to once more since this is considered a crucial reason for the extraordinary thermodynamic stability of this prominent framework. However, less attention has so far been attributed to the situation within the cavities of the anionic substructure, that is, the interaction of the latter with the counterions (**1**−**3**) and solvent molecules (**1**). As in the cited alkali metal salts,[25b,e] the K^+ ions and water molecules are disordered within the inner porous system that consists of two types of cavities which are located in the tetrahedral or octahedral holes of the open framework structure, respectively. They are connected via four identical, ellipse-shaped windows each with maximum diameters of 3.2 × 4.6 Å. In **1**, the larger cavity hosts two disordered water molecules (O2, O3), the third solvent molecule (O1) occupies the smaller cavity. Surprisingly, K^+ ions are not situated within the tetrahedral cages, but prefer the "bottle necks", that is, the positions on the triangular faces between the cages. This might be explained by the distinct preference for K···Se interactions (in comparison to K···O contacts)[30e] that are maximized this way: seven nearest K···Se contacts (356.4(12)−394.7(11) pm) stabilize the counterions on their positions, whereas the centers of the cavities would be by 393.4−499.6 pm (cage on octahedral hole position) or 436.9−438.9 pm (cage on tetrahedral hole position) away from the next Se position. For the ammonium salts **2** and **3**, the situation changes. Although the crystal structures of **2** and **3** show the same topology of M, T, and Se atoms as that of **1** (M = Mn, Fe; T = Ge, Sn) or the related compounds cited above, the network is naturally widened upon the substitution of Sn for Ge; the results are the center-to-next-Se distances of 429.3−640.9 (**2**), 430.9−667.8 (**3**) for cages on octahedral hole position, and 456.9−500.6 pm (**2**), 459.4−501.1 pm (**3**) for cages on the tetrahedral hole position, as well as window diameters of approximately 4.0 × 4.4 Å. The $[MSn_4Se_{10}]^{2-}$ substructures host $(NMe_4)^+$ cations that served as templates at the

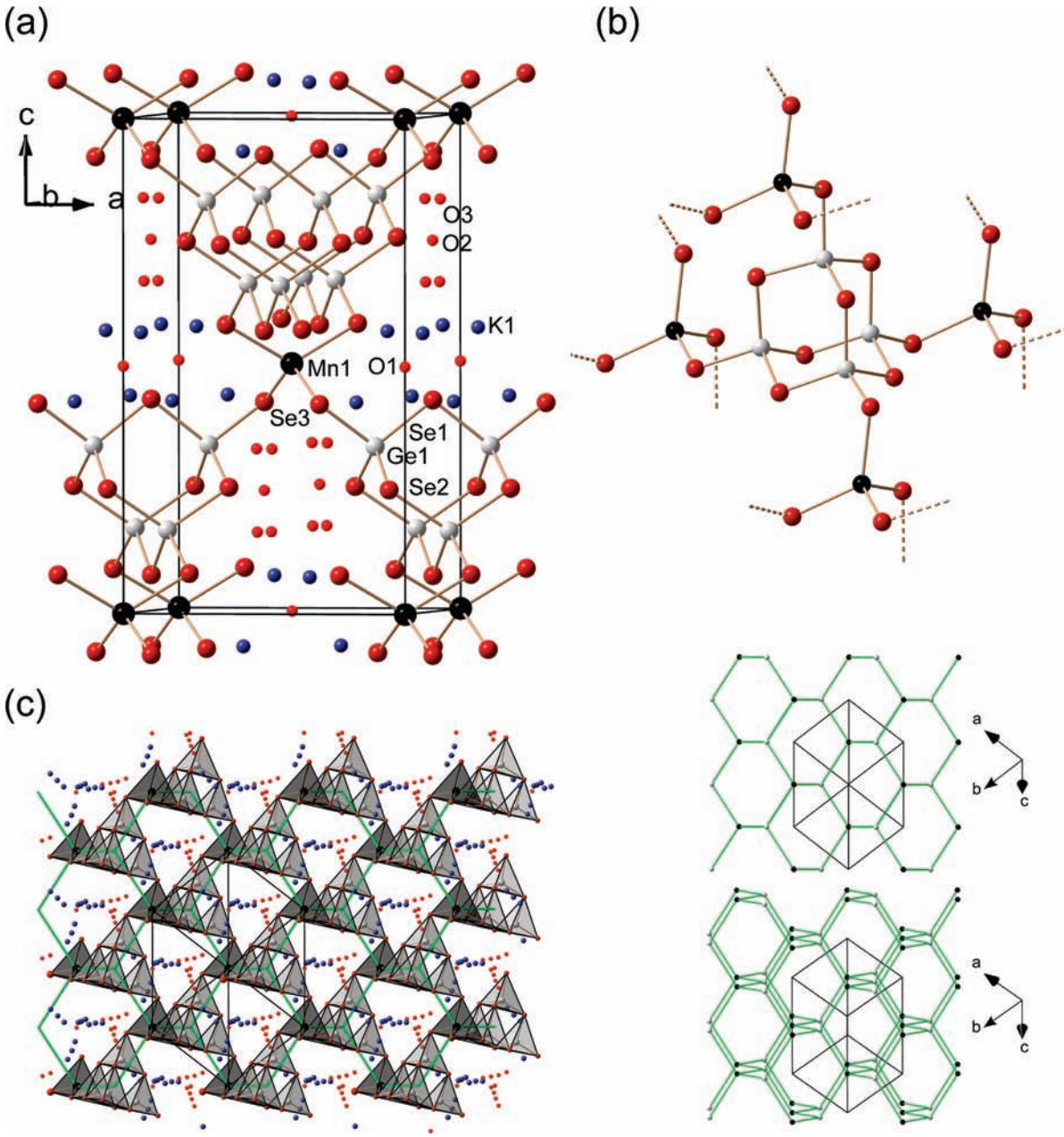

Figure 2. (a) Fragment of the crystal structure of **1** including all K and O split positions with site occupancy 0.35:0.07:0.07 (K1a−K1c) or 0.80:0.40:0.33:0.13 (O1, O2, O3a, O3b); (b) illustration of the near tetrahedral arrangement of corner-sharing $[Ge_4Se_{10}]^{4-}$ T2 units and $[MnSe_4]^{6-}$ T1 units; (c) polyhedral representation of the framework; the relationship to the diamond type topology is emphasized by green lines (right-hand side: different orientations) connecting T2 (gray) with T1 barycenters (black).

synthesis of the robust framework. Different from **1**, the (larger) cations are located within the cages (at 0,0,0 and 0,1/2,1/4), whereas the window positions are free. The (NMe_4) groups do not show any disorder, which can be put down on 12 or 10 Se···H bridges in the two cavities, respectively, enhancing the anion-cation interaction and thereby inhibiting any rotation of the methyl groups. The different structural features of **1** versus **2** and **3** correlate well with the conductivity behavior, as discussed below. Figure 3 illustrates the two types of counterion(/solvent) distributions within the related phases.

So far, attempts to construct the stannate network around (hydrated) K^+ cations, to probe the influence of different pore sizes on the ion mobility, failed under the given conditions because of the formation of salts of P1 cluster anions $[M_4Sn_4Se_{10}]^{10-}$ that represent another, highly advantaged structure type. Further variation of the reaction conditions and the use of different $[Sn_xSe_y]^{q-}$ anions as starting species might serve to overcome this problem.

Optical Absorption Behavior of 1 and 2. To rationalize the influence of different tetrel and/or transition metal atoms on the electronic excitation energies, compounds **1**−**3** have been investigated by means of UV−vis spectroscopy, recorded from suspensions of single crystals in nujol oil (Figure 4).

The optical absorption behavior of **1**−**3** shows similar characteristics, with a smooth onset of absorption followed by a number of band-type maxima, as expected somewhat more pronounced for the Fe compound **3**. The onset of

Table 2. Selected Interatomic Distances (pm) and Angles (deg) of the Crystallographically Characterized Compounds **1**−**4**[a]

compound	1	2	3	4
Ge−Se(−Mn)	229.41(12)			
Ge−Se(−Ge)	236.32(13)−237.62(13)			
Sn−Se−(M)		245.33(14)−254.11(14)	247.0(4)−255.1(3)	
Sn−Se−(Sn)		245.33(14)−254.11(14)	247.0(4)−255.1(3)	
Sn−Se_t		245.33(14)−254.11(14)	247.0(4)−255.1(3)	245.90(9)−258.71(10)
Mn−Se	254.98(9)	254.48(11)		
Fe−Se			246.6(3)	
K···O	253.5(17)−274.8(18)			
K···Se	356.4(12)−398.2(16)			
(N)H···Se		2.946(16)−3.753(14)	2.995(8)−3.806(11)	2.732(12)−3.992(11)
(O)H···Se				251.5(7)
Se−Ge−Se	102.74(5)−112.79(4)			
Ge−Se−Ge	103.60(5)−104.91(6)			
Se−Sn−Se		110.10(5)−112.21(4)	110.20(15)−112.22(12)	93.12(3)−113.65(3)
Sn−Se−Sn		104.50(7)−105.11(5)	104.54(14)−105.45(16)	86.88(3)
Se−Mn−Se	103.61(2)−121.96(5)	128.02(6)−101.07(2)		
Se−Fe−Se			102.27(5)−125.09(12)	
Ge−Se−Mn	107.33(4)		107.74(5)−111.76(14)	
Sn−Se−Mn		106.42(4)		
Sn−Se−Fe			107.44(12)	

[a] Distances within the coordination spheres of cations K^+ or $(NMe_4)^+$ are considered according to the given coordination numbers (c.n., see text) or as nearest distance N···Se.

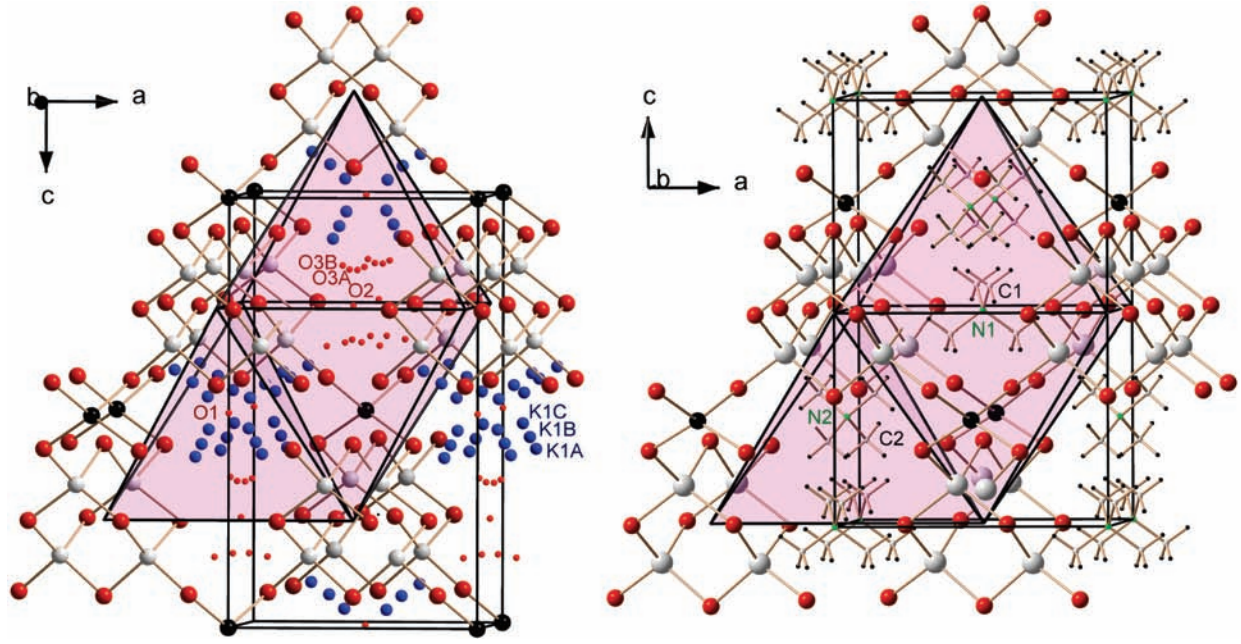

Figure 3. Occupation of inner cavities in **1** (left-hand side) and **2** (as an example for isostructural **2** and **3**, right-hand side). Disordered K^+ ions in **1** are located on the triangular faces connecting tetrahedral and octahedral cages [split positions on *x*, *y*, *z* = 0.3896(12), 0.729(2), 0.0985(9); 0.407(8), 0.655(8), 0.070(5); or 0.429(10), 0.592(6), 0.037(4), respectively], whereas N atoms of the $(NMe_4)^+$ ions occupy the centers of the octahedral and tetrahedral cages (*x*, *y*, *z* = 0,0,0 or 0,1/2,1/4, respectively).

absorption, that is, the lowest optical absorption energies of **1**, **2**, and **3** (approximately 1.9, 1.5, and 0.6 eV, respectively) are relatively small considering the visible color—even smaller than reported recently for spectra measured in the diffuse reflectance mode;[34] however, the absorption rises slowly and then becomes more significant at higher energies. According to the colors of the single crystals (Figure 1), the different absorption curves show increments of 0.6−1.0 eV in the visible part of the spectrum. The observations rationalize a significant contribution of an Se(p) → T(s,p) LMCT type excitation (T = tetrel atom Ge or Sn) in addition to a charge transfer involving Mn or Fe based d orbitals (MMCT or MLCT), as observed for $[K_{10}(H_2O)_{16.5}(MeOH)_{0.5}][Mn_4Sn_4Se_{17}]$.[28b]

Magnetism. To examine whether the paramagnetic ions in compounds like **1**−**3** would still magnetically interact with each other, we investigated a sample of single crystals of compound **1** by means of a magnetic susceptibility measurement.

At room temperature, the χT product is 4.4 $cm^3 \cdot K \cdot mol^{-1}$ in excellent agreement with the presence of only one Mn(II) atom ($S = 5/2$, $C = 4.375$ cm^3 K mol^{-1} with $g = 2$). When the temperature is lowered, the χT

(38) Roling, B. *Phys. Rev. B* **2000**, *61*, 5993.

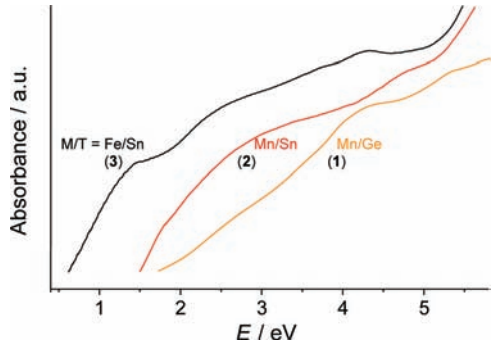

Figure 4. UV−vis spectra of **1**−**3**, recorded as suspensions of single crystals in nujol oil.

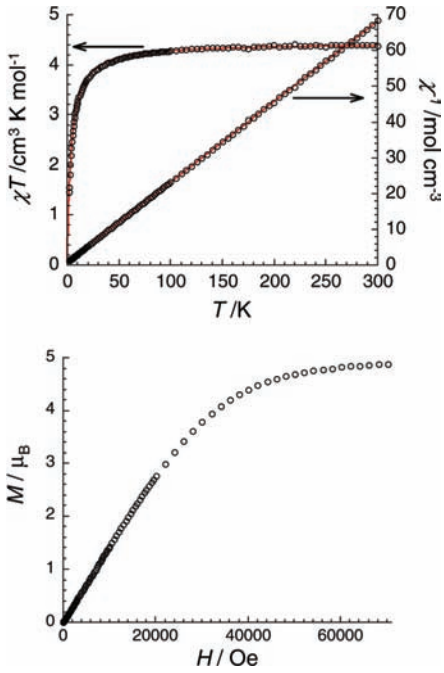

Figure 5. Top: χT and $1/\chi$ versus T plots from a polycrystalline sample of **1** measured under 1000 Oe (with $\chi = M/H$). The solid lines are the best fit obtained by a Curie−Weiss law as mentioned in the text. Bottom: M versus H plot obtained at 1.8 K.

product decreases continuously down to 1.4 $cm^3 \cdot K \cdot mol^{-1}$ at 1.8 K. The thermal magnetic behavior of **1** (top of Figure 5) indicates the presence of antiferromagnetic interactions between the $S = {}^5/_2$ spins at the Mn(II) centers within the structure. In the whole temperature range, the experimental data can be fitted to a Curie−Weiss law that leads to Curie and Weiss constants of 4.43 $cm^3 \cdot K \cdot mol^{-1}$ and −3.6 K, respectively. As the room temperature χT product, the Curie constant is in relatively good agreement with the presence of one Mn(II) metal ion as already mentioned above and as confirmed by the M versus H data at 1.8 K that saturate at about 5 μ_B (bottom of Figure 5). The negative Weiss constant is indicative of antiferromagnetic interactions between the spin carriers. For the 12 next Mn atoms around a given one that are arranged as a tetrahedrally elongated cuboctahedron (Figure 6) the strengths of the interaction can be estimated as $J/k_B = -50$ mK from the mean-field expression of the Weiss constant ($\theta = 2zJS(S + 1)/3k_B$ with z, the number of neighboring Mn^{II}, equal to 12, $S = 5/2$).

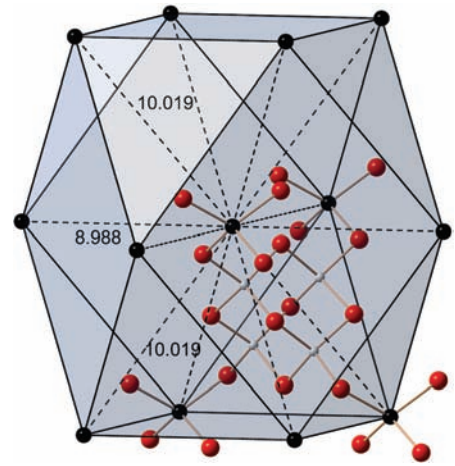

Figure 6. Illustration of the non-bonding arrangement of magnetically interacting Mn(II) centers in **1**. Distances to the next Mn atoms are given in angstrom.

In **2** or **3**, respectively, the M···M distances are larger (**2**: 9.865, 10.359 Å; **3**: 9.878, 10.376 Å) as to be expected for the stannate network. Therefore, one can presume the magnetic interactions to be even weaker than in **1**.

Conductivity Measurements and Thermal Behavior of 1 and 2. Intending to gain insight into ion mobility and conductivity characteristics of the K^+ versus $(NMe_4)^+$ containing phases, we performed impedance spectroscopic measurements of pellets of single crystals of **1** and **2**. From the frequency-dependent complex impedance of the samples, $\hat{Z}(\nu) = Z'(\nu) - i \cdot Z''(\nu)$, the real part of the conductivity $\sigma'(\nu)$ was calculated according to

$$\sigma'(\nu) = \frac{d}{A} \cdot \frac{Z'(\nu)}{[Z'(\nu)]^2 + [Z''(\nu)]^2} \qquad (2)$$

Here, d and A denote the thickness and the area of the sample, respectively. At sufficiently high temperatures, the $\sigma'(\nu)$ spectra were characterized by low-frequency plateaus. In this plateau regime, the conductivity is identical to the bulk dc conductivity σ_{dc}, reflecting long-range ion transport in the sample.[38] Figure 7 shows the Arrhenius plots for the bulk dc conductivities σ_{dc} of both materials; Figure 8 gives the thermal gravimetric analyses results of both compounds (note that crystals of **1** were dried prior to the measurements).

Between 40 and 220 °C, the data of the K^+ ion containing coordination polymer **1** follow an Arrhenius law

$$\sigma_{dc} = \sigma_0 \exp(-E_A/k_B T) \qquad (3)$$

with an activation energy of $E_A = 0.78$ eV. Below 40 °C, dc conductivity plateaus could not be detected. Above 220 °C, the conducting polymer EMI-tec AS61 decomposes and cannot be used anymore as electrode material. However, the

(39) (a) Depemeier, W.; Möller, A.; Klaska, K.-H. *Acta Crystallogr.* **1980**, *B36*, 803–807. (b) Hollemann, A. F.; Wiberg, E.; Wiberg, N. *Lehrbuch der Anorganischen Chemie*, 102nd ed.; deGruyter: Berlin, NY, 2007; p 2003.
(40) Wilmer, D.; Feldmann, H.; Lechner, R. E.; Combet, J. *J. Mater. Res.* **2005**, *20*, 1973.
(41) Witschas, M.; Eckert, H.; Freiheit, H.; Putnis, A.; Korus, H.; Jansen, M. *J. Phys. Chem. A* **2001**, *105*, 6808.

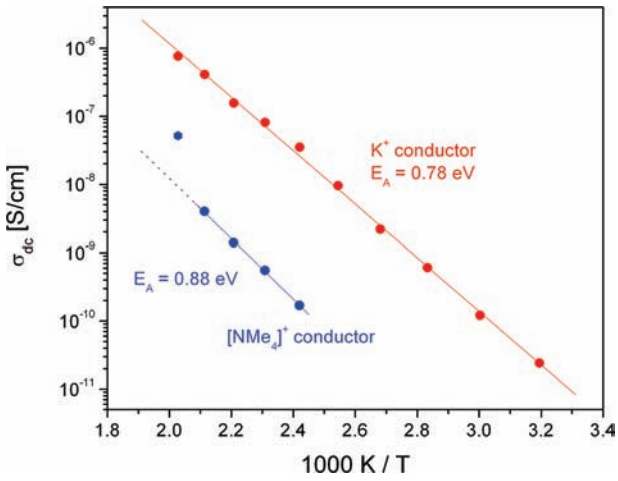

Figure 7. Arrhenius plot for the dc conductivity σ_{dc} of **1** (red data and fit) and **2** (blue data and fit).

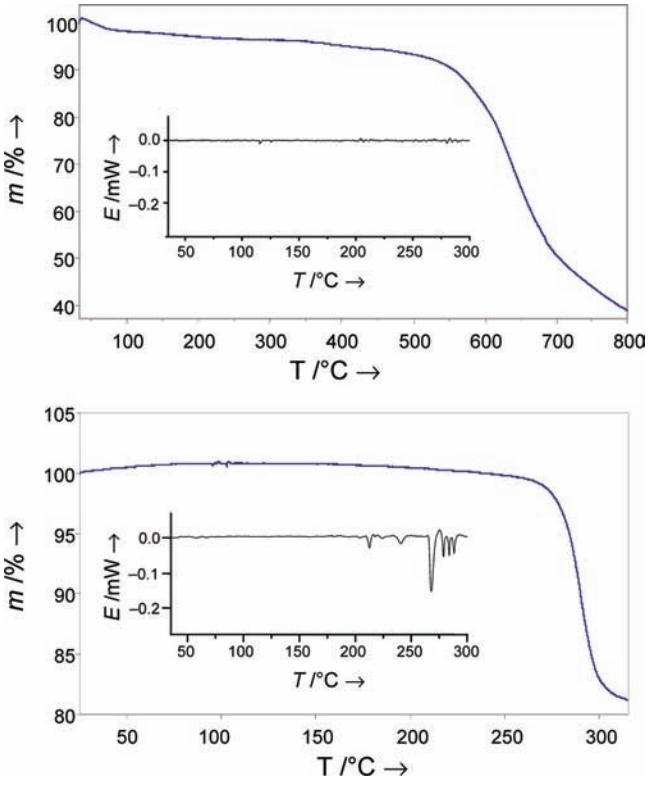

Figure 8. Results of the TGA measurements (large figure: DTA; zoom: cutout of the DSC measurement between 30−300 °C) of dried **1** (35−800 °C, top) and **2** (25−310 °C, bottom).

TGA measurements show that the phase is thermally stable up to 550 °C, which exceeds the thermal stability of all of the corresponding ammonium salts reported so far and also seems more robust than $Cs_2[FeGe_4S_{10}]\cdot xH_2O$.[25b] A comparison of the ion conductivity of **1** with those of the analogous Rb^+ or Cs^+ salt has not been possible so far because of the lack of corresponding data.

In comparison to the K^+ ion containing coordination polymer, the $(NMe_4)^+$ polymer exhibits both lower conductivity and thermal stability. Lower conductivity is expected since the ionic radius of $(NMe_4)^+$ (r = 230 pm)[39a] is larger than the radius of the K^+ ion (r = 152 pm for c.n. = 6).[39b] The dc conductivity plateaus were detectable at temperatures ≥140 °C. In a temperature range between 140 and 200 °C, the dc conductivity exhibits Arrhenius behavior with an activation energy of E_A = 0.88 eV. Above 200 °C we detect deviations from Arrhenius behavior with a conductivity being higher than expected from the extrapolation of the Arrhenius fit. In the DSC measurements, we find an endothermic process at about 210 °C, which is presumably caused by the onset of rotational movements of the $(NMe_4)^+$ ions. Apparently, this dynamic process leads to a change in the effective interactions between the $(NMe_4)^+$ ions and polymer matrix and, therefore, to a change in the mobility of the $(NMe_4)^+$ ions. It is well-known that in plastic crystals, such as Na_3PO_4, rotational movements of the anions exhibit a strong influence on the translational diffusion of the cations.[40] Much less is known about crystals with the same type of ion carrying out both translational and rotational movements. Therefore, coming investigation will include dynamic studies on the $(NMe_4)^+$ compound using quasi-elastic neutron scattering[40] and solid-state NMR techniques.[41] The decomposition above 280 °C comes along with a weight loss of roughly 18%, which is a little more than calculated for the simple decomposition reaction evolving solid $MnSn_4Se_9$ upon the release of 1 equiv of Me_2S and 2 equiv of NMe_3 per formula unit (12.3%).[25d] Obviously, the collapse of the compound is more complicated in this case.

Conclusion and Outlook

Three new phases that are based on open framework compounds of the type $\{[MT_4E_{10}]^{2-}\}_n$ were synthesized and characterized by means of single crystal X-ray diffractometry as well as optical absorption spectroscopy. The phases represent the first stannate homologues of known $(NMe_4)^+$ containing germanates, as well as the germanate salt with K^+ as the smallest cation type observed so far in these phases. The systems exhibit a diamond topology with a corresponding 3D pore structure hosting the counterion/solvent aggregate and possess band gaps in the visible to near-infrared region. In spite of the channel structure, ion mobility and conductivity studies have not been discussed so far. To shed light on the latter, we investigated the K^+ salt as a benchmark and the $(NMe_4)^+$ containing stannate as a reference by impedance spectroscopy. Indeed, the conductivity in the K^+ phase is higher, features a relatively high thermal stability up to 600 °C, and exhibits typical Arrhenius behavior with an activation energy of 0.78 eV. This corresponds to values of moderate ion conductors and shows the potential of these chalcogenide phases for the combination of various physical properties: here medium energy optical absorption and ion conductivity. In addition, we detected magnetic interactions between Mn^{2+} ions within the germanate phase although they are separated by $[Ge_4Se_{10}]^{4-}$ units at a distance of approximately 10 Å. The findings prompt a number of future investigations, including the ongoing exchange of Na^+ or even Li^+ for K^+ within the framework, with a so far unknown impact on the ion conductivity,

together with further variation of the components to create ion conducting semiconductors for applications such as sensors or directed ion conductivity. Another concern is the different behavior of ammonium versus alkali metal salts within porous network structures which will help to understand and design novel ion conductors.

Acknowledgment. This work was financially supported by the German Science Foundation (Deutsche Forschungsgemeinschaft, DFG). We are very grateful to F. Schmock for valuable help. We also thank the University of Bordeaux, the CNRS, and the Région Aquitaine for financial support. We thank J. Hehl for the DTG/DSC measurements.

Supporting Information Available: Further details are given in crystallographic information files (CIF). This material is available free of charge via the Internet at http://pubs.acs.org.

IC802170F